AIMS Mathematics

https://www.aimspress.com/journal/Math

AIMS Mathematics, 10(8): 17334–17361.
DOI: 10.3934/math.2025775
Received: 10 April 2025
Revised: 04 July 2025
Accepted: 24 July 2025
Published: 01 August 2025

Research article

Bayesian and classical inference for a novel model: medical and economical real data analysis

Muqrin A. Almuqrin[1,*] **and Mohammed AbaOud**[2]

[1] Department of Mathematics, College of Science in Zulfi, Majmaah University, Majmaah 11952, Saudi Arabia
[2] Department of Mathematics and Statistics, Imam Mohammad Ibn Saud Islamic University (IMSIU), Riyadh 11564, Saudi Arabia

* **Correspondence:** Email: m.almuqrin@mu.edu.sa.

Abstract: In the literature on distribution theory, numerous probability distributions are applied to predict and model real-world phenomena across diverse applied domains, including the medical and healthcare sectors. In the present paper, we develop a new distributional method, referred to as the new exponential power function distribution. The introduced model is incorporated using the transformed-transformer (T-X) approach. The density function of the newly presented distribution is investigated graphically, revealing three distinct patterns, namely symmetric, asymmetric, complex, and skewed shapes. Similarly, the hazard function patterns of the proposed model are also illustrated, which capture the increasing, unimodal, decreasing, and increasing shapes. Further, we developed several key properties such as the moments, quantile function, moment-generating function, and order statistics. Several classical and Bayesian estimation parameters of the new distribution are provided. A Monte Carlo simulation study is conducted to assess the efficiency of these estimators. Lastly, the practicality and efficiency of the novel distribution were validated using four datasets. It is found that the proposed distribution efficiently analyzed these datasets compared with competitive distributions.

Keywords: Bayes estimator; financial; hazard rate function; T-X approach; symmetric
Mathematics Subject Classification: 60B12, 62G30

1. Introduction

In recent years, the generalization of existing well-known distributions has been trending to accommodate more flexibility in the existing distributions by incorporating additional parameters in the model. Data analysis has long been a focus for researchers, particularly in the context of probabilistic reasoning and quantification. Probability models are valuable tools in numerous disciplines, including engineering, biology, environmental sciences, insurance, actuarial sciences, and medical sciences. These probability models facilitate describing, modeling, and forecasting the time until an event of interest, such as system failure, illness remission, or product lifetime.

To bring further flexibility to these generated distributions, various approaches of well-known models have been defined and used in several applied sciences. For example, Amal et al. [1] proposed the inverse Weibull-G model. Meraou et al. [2, 3] considered the compound exponential and gamma models to bring further flexibility to these generated distributions. Alzaatreh et al. [4] suggested the T-X family models. Further, Thomas et al. [5] introduced the power generalized Dinesh Umesh Sanjay (DUS) distribution. Meraou et al. [6] established a compound maximum Poison log-normal model. Eugene et al. [7] provided the beta-normal model. Cordeiro et al. [8] defined the Kumaraswamy-G family. Along the same lines, Marshall and Olkin [9] proposed a novel technique for generating a new class of distributions, and Almetwally and Meraou [10] developed the sine Nadaraja Haghighi model. Ahmad et al. [11] proposed a new distributional method: A new family of heavy-tailed distributions. Another new helpful approach for modifying the existing distributions pioneered by Ahmad et al. [12] is called, the weighted T-X family. He et al. [13] also introduced a novel method for generalizing the traditional distributions by implementing a trigonometric function called the arcsine exponentiated-X family.

However, the authors found no flexible probability distribution in the literature that accommodates every phenomenon because phenomena are complex. As a result, researchers have increasingly focused on defining novel approaches to probability distributions to increase the versatility levels of classical distributions. These efforts involve incorporating one or more extra parameters into the baseline distribution, which improves the flexibility level of the resulting distribution in modeling and predicting various types of data in practice. In this regard, an important modification to a well-known distribution named the new exponential (NE) class of distributions is used. The proposed transformation is based on the T-X method, and it can be described as follows. Let $k(y)$ be the probability density function (PDF) of a random variable $Y \in [a_1, a_2]$ and let $W[M(t)]$ be a function of the cumulative distribution function (CDF) of a random variable T which satisfies the conditions bellow: (1) $W[M(t)] \in [a_1, a_2]$; (2) $W[M(t)]$ is differentiable and monotonically non decreasing; (3) $\lim_{t\to-\infty} W[M(t)] = a_1$ and $\lim_{t\to\infty} W[M(t)] = a_2$.

Consequently, the CDF and the corresponding PDF of the T-X technique can be written as follows:

$$\Lambda(x) = \int_{a_1}^{W[M(t)]} k(y)dy,$$

and

$$\lambda(x) = \left\{\frac{d}{dx} W[M(t)]\right\} r(W[M(t)]).$$

Here in this study, we chose

$$W[M(t)] = -\log\left\{(1 - G(y;\xi))\, e^{-\theta G(y,\xi)}\right\},$$

and the random variable Y has the exponential distribution with the parameter 1. Further, the corresponding CDF and PDF of the NE class of distributions are

$$\Lambda(y;\xi,\theta) = 1 - [1 - G(y;\xi)]\ e^{-\theta G(y,\xi)} \quad y \in \mathbb{R}, \quad \theta > 0, \tag{1.1}$$

and

$$\lambda(y;\xi,\theta) = g(y;\xi)\ [1 + \theta G(y;\xi)]\ e^{-\theta G(y,\xi)}. \tag{1.2}$$

It is well documented that the NE tool has garnered scholarly interest due to their mathematical tractability and flexibility. It has a wider applications in biology, health sciences, hydrology, medical sciences, finance, and other fields. This latest modification introduces one additional parameter in a baseline distribution and it has the ability to model different kinds of data sets, and its CDF and PDF have closed formulas.

Recently, Meniconi and Barry [14] considered the power distribution (PD). Its applications extend to modeling survival, household income, and insurance claims. The idea behind choosing the PD as a special member is that it has proven to be suitable for modeling economic phenomena and other connected sectors, including biological, actuarial science, and survival analysis for mortality rates. Additionally, it is frequently used to model the upper tail of disease severity data, which is essential for identifying worst-case scenarios in epidemiological studies. Some extensions of the PD have been considered. Among these models, ElSherpieny and Almetwally [15] introduced the exponentiated generalized alpha power family with economic data set, Wang and Zhu [16] demonstrated the effectiveness of the extension for PD in modeling engineering datasets, Almongy et al. [17] discussed the Marshall_Olkin alpha power Lomax distribution for physical datasets, while Alshawarbeh et al. [18] utilized it for fitting medical science applications, and Elsherpieny et al. [19] discussed the alpha-power exponential distribution using unified hybrid censored data. In reliability and survival studies, a new approach to PD has been considered in different studies, including Muhi et al. [20]. In particular, the PD can be regarded as a limiting distribution for residual lifetimes, as elucidated by [21–23]. The continuous random variable X is said to have the PD if it has a CDF given by

$$\Pi(x;\alpha,\beta) = \left(\frac{x}{\beta}\right)^{\alpha},\ 0 < x < \beta,\ \alpha,\beta > 0. \tag{1.3}$$

The PDF corresponding to Eq (1.3) can be obtained through the following formula:

$$\pi(x;\alpha,\beta) = \frac{\alpha\ x^{\alpha-1}}{\beta^{\alpha}}. \tag{1.4}$$

In this work, we derive a more flexible PD by inserting the standard baseline PD into a flexible family using the exponential transformed technique. The model thus obtained is known as the exponential power distribution (EPD). The supplementary parameter offers increased versatility in analyzing the tail behavior of the specified density function. The proposed model offers greater flexibility compared with other versions of the PD. Since the proposed model captures tail behavior effectively, it is particularly useful in understanding the upper quantiles of life expectancy or survival time, often related to elderly patients or those undergoing life-extending treatments. For more information, see the works of [24–26]. This modeling helps predict severe complications in patients with critical conditions of certain diseases, such as COVID-19 and heart disease. As a result, the proposed EPD is more appropriate to fit failure times or the time to extreme events, such as treatment failure or device malfunction. Henceforth, in this study, we estimate the unknown parameters for the recommended EPD by two several estimation techniques, notably, the maximum likelihood estimator (MLE) and the Bayes method; see, for example, [27,28].

The key motivations of this study include the following:

- The EPD is particularly valuable in various fields where skewed distributions are prevalent.
- The EPD can have a reverse-J-shaped or inverted bathtub-shaped hazard rate, which can be seen in most real-world situations and is extremely effective in reliability analyses.
- A paramount goal of the EPD is to fit left_skewed, right_skewed, and even complex data so this model outfits all it base line models.
- The EPD excels in constructing heavy-tailed densities that are not excessively long-tailed, striking a balance between tail behavior and computational tractability. This characteristic is essential for accurately modeling various real-life datasets characterized by heavy-tailed distributions, such as income and wealth data, extreme event occurrences, and environmental phenomena. By providing a realistic representation of tail behavior, the EPD enhances the reliability and robustness of statistical analyses.

The remainder the study is organized as follows. The EPD is introduced in Section 2. We derive and discuss its key theoretical characteristics in Section 3. Two different estimation approaches are discussed in Section 4. A detailed simulation study is performed in Section 5. Four different datasets are analyzed in Section 6, and concluding remarks are proved in Section 7.

2. The construction of the EDP

Here, we develop the distributional properties of the proposed EPD, and numerous graphic illustrations of these functions are examined. Now, consider a random variable Z that follows the EPD. By using Eqs (1.1)–(1.3), the CDF of Z is

$$\Phi(z;\alpha,\beta,\theta) = 1 - \left(1 - \left(\frac{z}{\beta}\right)^{\alpha}\right) e^{-\theta\left(\frac{z}{\beta}\right)^{\alpha}}, \quad 0 < z < \beta, \quad \alpha,\beta,\theta > 0. \tag{2.1}$$

Corresponding to $\Phi(z;\alpha,\beta,\theta)$ of the EPD, the PDF $\phi(z;\alpha,\beta,\theta)$ of Z, is given by

$$\phi(z;\alpha,\beta,\theta) = \frac{\alpha z^{\alpha-1}}{\beta^{\alpha}} \left[1 + \theta\left(\frac{z}{\beta}\right)^{\alpha}\right] e^{-\theta\left(\frac{z}{\beta}\right)^{\alpha}}. \tag{2.2}$$

From Eq (2.1), the parameter α controls the scale of the distribution while the parameter θ controls its shape. We also immediately obtain$\lim_{z\mapsto 0} \Phi(z;\alpha,\beta,\theta) = 0$ and $\lim_{z\mapsto\infty} \Phi(z;\alpha,\beta,\theta) = 1$.

Next, we present the density and CDF curves in Figures 1 and 2, respectively, of the EPD using numerous selected parameter values. It has unimodal, increasing, and decreasing structures for specific parameter combinations. This ensured that the recommended EPD is more suitable for modeling several kinds of datasets.

Furthermore, the survival function (SF) and hazard rate function (HRF) of the EPD are given below:

$$S(z;\alpha,\beta,\theta) = \left(1 - \left(\frac{z}{\beta}\right)^{\alpha}\right) e^{-\theta\left(\frac{z}{\beta}\right)^{\alpha}},$$

and

$$h(z;\alpha,\beta,\theta) = \frac{\alpha z^{\alpha-1}\left[1 + \theta\left(\frac{z}{\beta}\right)^{\alpha}\right]}{\beta^{\alpha}\left[1 - \theta\left(\frac{z}{\beta}\right)^{\alpha}\right]}.$$

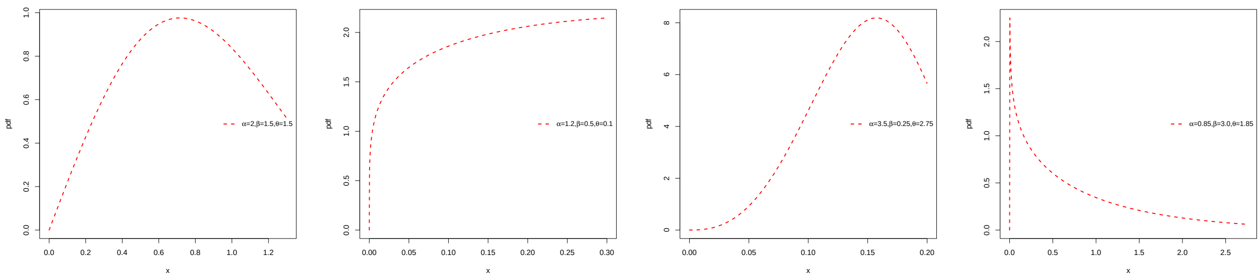

(a) (2,1.5,1.5) **(b)** (1.2,0.5,0.1) **(c)** (3.5,0.25,2.75) **(d)** (0.85,3,1.85)

Figure 1. A graphical illustration of $\phi(z;\alpha,\beta,\theta)$ of the EPD.

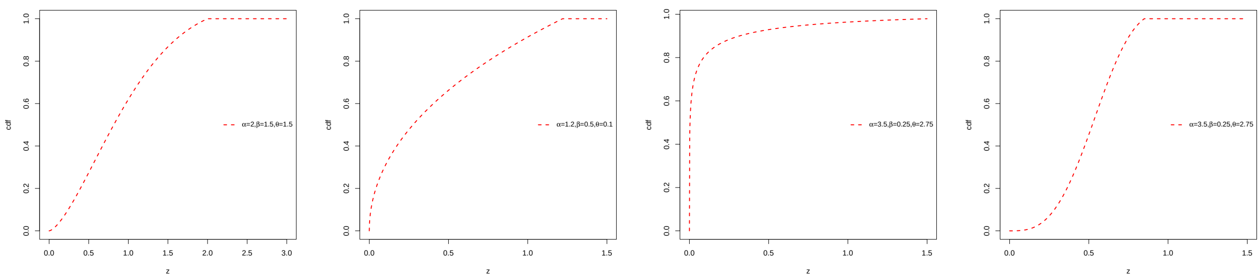

(a) (2,1.5,1.5) **(b)** (1.2,0.5,0.1) **(c)** (3.5,0.25,2.75) **(d)** (0.85,3,1.85)

Figure 2. A graphical illustration of $\Phi(z;\alpha,\beta,\theta)$ of the EPD.

Figures 3 and 4 illustrate, respectively, the hazard and survival function plots for the EPD. The HRF has increasing, decreasing, and unimodal shapes. This indicates that the hazard rate consistently increases and decreases over time without significant fluctuations.

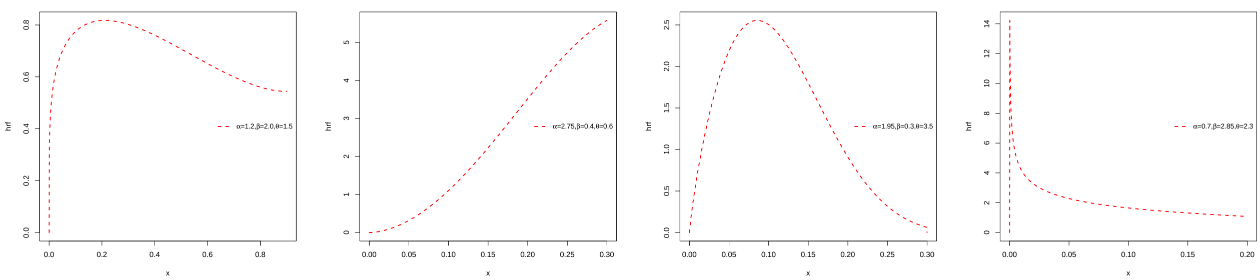

(a) (1.2,2,1.5) **(b)** (2.75,0.4,0.6) **(c)** (1.95,0.3,3.5) **(d)** (0.7,2.85,2.3)

Figure 3. A graphical illustration of $h(z;\alpha,\beta,\theta)$ of the EPD.

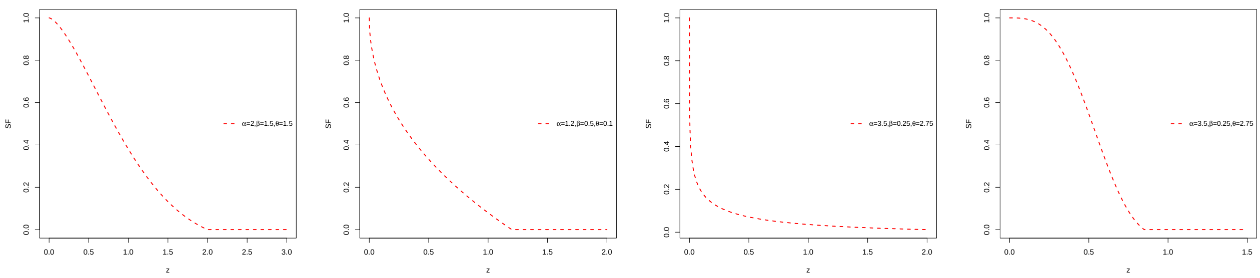

(a) (1.2,2,1.5) **(b)** (2.75,0.4,0.6) **(c)** (1.95,0.3,3.5) **(d)** (0.7,2.85,2.3)

Figure 4. A graphical illustration of $S(z;\alpha,\beta,\theta)$ of the EPD.

3. Mathematical properties of the EPD

3.1. Quantile function

This part aims to clarify specific quartiles-based properties of the EPD. The aspects to be analyzed consist of the quantile function (QF), the calculation of quartiles, and the measures of skewness and kurtosis. If Z is a random variable of the EPD, then the quantile function of order u can be defined as

$$z_u = \beta\left\{1 - \frac{1}{\theta} W\left[\theta\, e^{\theta}(1-u)\right]\right\}^{\frac{1}{\alpha}}, \quad 0 < u < 1, \tag{3.1}$$

where $W(.)$ is the positive branch Lambert function.

Proof. The QF of Z is written as

$$1 - \left(1 - \left(\frac{z}{\beta}\right)^{\alpha}\right) e^{-\theta\left(\frac{z}{\beta}\right)^{\alpha}} = u, \qquad \left(1 - \left(\frac{z}{\beta}\right)^{\alpha}\right) e^{-\theta\left(\frac{z}{\beta}\right)^{\alpha}} = 1 - u.$$

Multiplying by e^{θ}, we obtain

$$\left(1 - \left(\frac{z}{\beta}\right)^{\alpha}\right) e^{-\theta\left(\frac{z}{\beta}\right)^{\alpha}+\theta} = e^{\theta}(1-u). \tag{3.2}$$

Now, we multiply the equation above by θ. Equation (3.2) can be rewritten as

$$\theta\left(1 - \left(\frac{z}{\beta}\right)^{\alpha}\right) e^{-\theta\left(\frac{z}{\beta}\right)^{\alpha}+\theta} = \theta e^{\theta}(1-u), \qquad \theta\left(1 - \left(\frac{z}{\beta}\right)^{\alpha}\right) e^{\theta\left(1-\left(\frac{z}{\beta}\right)^{\alpha}\right)} = \theta e^{\theta}(1-u).$$

As a result,

$$\theta\left(1 - \left(\frac{z}{\beta}\right)^{\alpha}\right) = W\left[\theta e^{\theta}(1-u)\right],$$
$$1 - \left(\frac{z}{\beta}\right)^{\alpha} = \frac{1}{\theta}\, W\left[\theta e^{\theta}(1-u)\right],$$

$$\left(\frac{z}{\beta}\right)^{\alpha} = 1 - \frac{1}{\theta}\, W\left[\theta e^{\theta}(1-u)\right],$$

$$z = \beta\left\{1 - \frac{1}{\theta} W\left[\theta\, e^{\theta}(1-u)\right]\right\}^{\frac{1}{\alpha}}.$$

Now, if we take $u = \frac{1}{2}$, we can be deduced the value of the median, which is given below

$$z_{0.5} = \beta\left\{1 - \frac{1}{\theta} W\left[\frac{1}{2}\,\theta e^{\theta}\right]\right\}^{\frac{1}{\alpha}}.$$

Additionally, the Bowleys skewness (SK) and Moors kurtosis (KR) of the EPD are described as

$$SK = \frac{z_{0.25} + z_{0.75} - 2z_{0.5}}{z_{0.75} - z_{0.25}},$$

and

$$KR = \frac{z_{0.875} - z_{0.625} + z_{0.375} - z_{0.125}}{z_{0.75} - z_{0.25}}.$$

□

3.2. Moment

Let Z be the EPD with the PDF $\phi(z;\alpha,\beta,\theta)$ in Eq (2.2). In this case, the kth moment of Z is given below

$$u'_k = \frac{\beta^k}{\theta^{1+\frac{k}{\alpha}}}\left\{\Gamma\left(\frac{k}{\alpha}+1\right) + \Gamma\left(\frac{k}{\alpha}+2\right)\right\}. \tag{3.3}$$

Proof. The kth-moment of Z can be defined as

$$\begin{aligned} u'_k &= \int_0^{\infty} z^k\, \phi(z;\alpha,\beta,\theta)\, dz \\ &= \int_0^{\infty} z^k\, \frac{\alpha z^{\alpha-1}}{\beta^{\alpha}}\left[1 + \theta\left(\frac{z}{\beta}\right)^{\alpha}\right] e^{-\theta\left(\frac{z}{\beta}\right)^{\alpha}}\, dz \\ &= \frac{\alpha}{\beta^{\alpha}}\int_0^{\infty} z^{\alpha+k-1}\left[1 + \theta\left(\frac{z}{\beta}\right)^{\alpha}\right] e^{-\theta\left(\frac{z}{\beta}\right)^{\alpha}}\, dz. \end{aligned}$$

Let $t = \left(\frac{z}{\beta}\right)^{\alpha}$, in which case, $z = \beta t^{\frac{1}{\alpha}}$ and $dz = \frac{\beta}{\alpha} t^{\frac{1}{\alpha}-1}\, dt$. Consequently

$$\begin{aligned} u'_k &= \frac{\alpha}{\beta^{\alpha}}\int_0^{\infty} (\beta t^{\frac{1}{\alpha}})^{\alpha+k-1}\, (1+\theta t)\, e^{-\theta t}\, \frac{\beta}{\alpha} t^{\frac{1}{\alpha}-1}\, dt \\ &= \beta^k \int_0^{\infty} t^{\frac{k}{\alpha}}\, (1+\theta t)\, e^{-\theta t}\, dt \\ &= \beta^k\left[\int_0^{\infty} t^{\frac{k}{\alpha}}\, e^{-\theta t}\, dt + \theta\int_0^{\infty} t^{\frac{k}{\alpha}+1}\, e^{-\theta t}\, dt\right] \end{aligned}$$

$$= \frac{\beta^k}{\theta^{1+\frac{k}{\alpha}}} \left\{ \Gamma\left(\frac{k}{\alpha}+1\right) + \Gamma\left(\frac{k}{\alpha}+2\right) \right\}.$$

Based on Eq (3.3), the mean and variance of the EPD are

$$E(Z) = \frac{\beta}{\theta^{\frac{1}{\alpha}+1}} \left\{ \Gamma\left(\frac{1}{\alpha}+1\right) + \Gamma\left(\frac{1}{\alpha}+2\right) \right\},$$

and

$$V(Z) = \frac{\beta^2}{\theta^{\frac{2}{\alpha}+1}} \left\{ \Gamma\left(\frac{2}{\alpha}+1\right) + \Gamma\left(\frac{2}{\alpha}+2\right) - \frac{1}{\theta}\left[\Gamma\left(\frac{1}{\alpha}+1\right) + \Gamma\left(\frac{1}{\alpha}+2\right) \right]^2 \right\}.$$

Finally, the dispersion index of Z is $ID = \dfrac{V}{u_1'}$.

Ultimately, the moment generating functions (MGF) can be used to estimate the moments, if they exist in the mathematical sense. The MGF of Z, say $M(t)$, can be expressed as shown below:

$$\begin{aligned} M(t) &= \int_0^\infty e^{tz}\phi(z;\alpha,\beta,\theta)\,dz = \sum_{k=0}^\infty \frac{t^k}{k!} z^k \phi(z;\alpha,\beta,\theta)\,dz \\ &= \sum_{k=0}^\infty \frac{t^k}{k!} u_k' = \sum_{k=0}^\infty \frac{t^k \beta^k}{k!\,\theta^{1+\frac{k}{\alpha}}} \left\{ \Gamma\left(\frac{k}{\alpha}+1\right) + \Gamma\left(\frac{k}{\alpha}+2\right) \right\}. \end{aligned} \tag{3.4}$$

□

Tables 1 and 2 compile some key statistical measures of the EPD, showcasing various choices of the parameters α, β, and θ. Where Figures 5 and 6 are the three dimensional curves of these statistical properties of the proposed model.

Table 1. Numerical values of different statistical measures of the EPD at $\theta = 1.3$.

	β	μ_1'	V	ID	SK	KR
α=0.25	0.2	0.0225	0.0016	1.7615	2.3936	5.384
	0.4	0.0451	0.0063	1.7615	2.3936	5.384
	0.6	0.0676	0.0142	1.7615	2.3936	5.384
	0.8	0.0901	0.0252	1.7615	2.3936	5.384
α=0.5	0.2	0.0470	0.0023	1.0201	1.3226	0.9020
	0.4	0.0940	0.0092	1.0201	1.3226	0.9020
	0.6	0.1410	0.0207	1.0201	1.3226	0.9020
	0.8	0.1880	0.0368	1.0201	1.3226	0.9020
α=0.75	0.2	0.0680	0.0024	0.7173	0.8747	-0.2056
	0.4	0.1360	0.0095	0.7173	0.8747	-0.2056
	0.6	0.2040	0.0214	0.7173	0.8747	-0.2056
	0.8	0.2720	0.0381	0.7173	0.8747	-0.2056
α=1.0	0.2	0.0849	0.0022	0.5521	0.6302	-0.6182
	0.4	0.1697	0.0088	0.5521	0.6302	-0.6182
	0.6	0.2546	0.0198	0.5521	0.6302	-0.6182
	0.8	0.3395	0.0351	0.5521	0.6302	-0.6182

Table 2. Numerical values of different statistical measures of the EPD at $\theta = 2$.

	β	μ'_1	V	ID	SK	KR
α=0.25	0.2	0.0225	0.0014	1.6364	2.5043	6.2577
	0.4	0.0451	0.0054	1.6364	2.5043	6.2577
	0.6	0.0676	0.0122	1.6364	2.5043	6.2577
	0.8	0.0901	0.0217	1.6364	2.5043	6.2577
α=0.5	0.2	0.0514	0.0019	0.8404	1.3996	1.3026
	0.4	0.1028	0.0075	0.8404	1.3996	1.3026
	0.6	0.1542	0.0168	0.8404	1.3996	1.3026
	0.8	0.2055	0.0298	0.8404	1.3996	1.3026
α=0.75	0.2	0.0754	0.0018	0.5574	0.9983	0.1707
	0.4	0.1507	0.0071	0.5574	0.9983	0.1707
	0.6	0.2261	0.0159	0.5574	0.9983	0.1707
	0.8	0.3015	0.0282	0.5574	0.9983	0.1707
α=1.0	0.2	0.0936	0.0015	0.4156	0.7960	-0.2637
	0.4	0.1872	0.0061	0.4156	0.7960	-0.2637
	0.6	0.2808	0.0136	0.4156	0.7960	-0.2637
	0.8	0.3745	0.0242	0.4156	0.7960	-0.2637

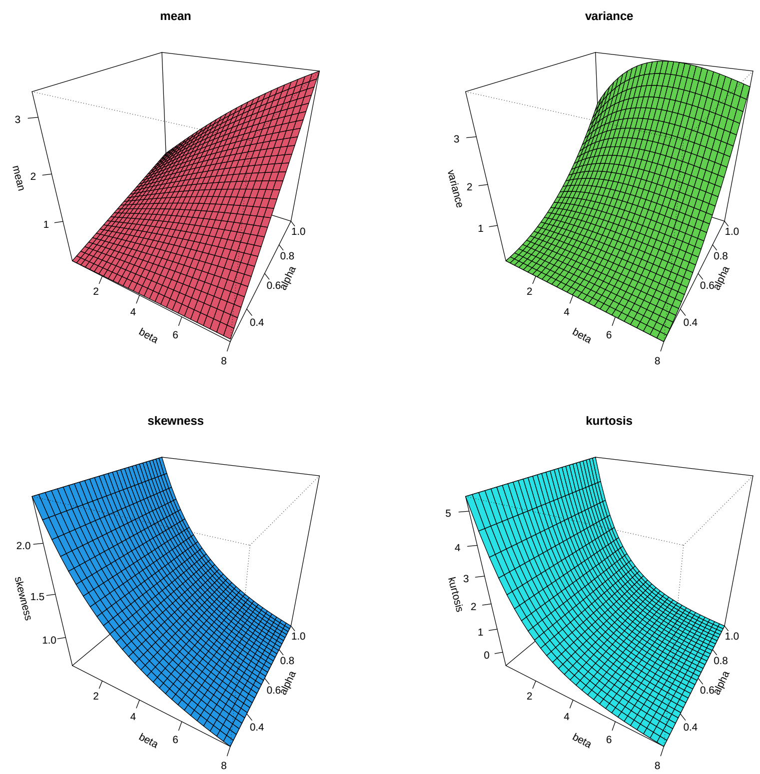

Figure 5. Mathematical properties plots of the EPD at $\theta = 1.3$.

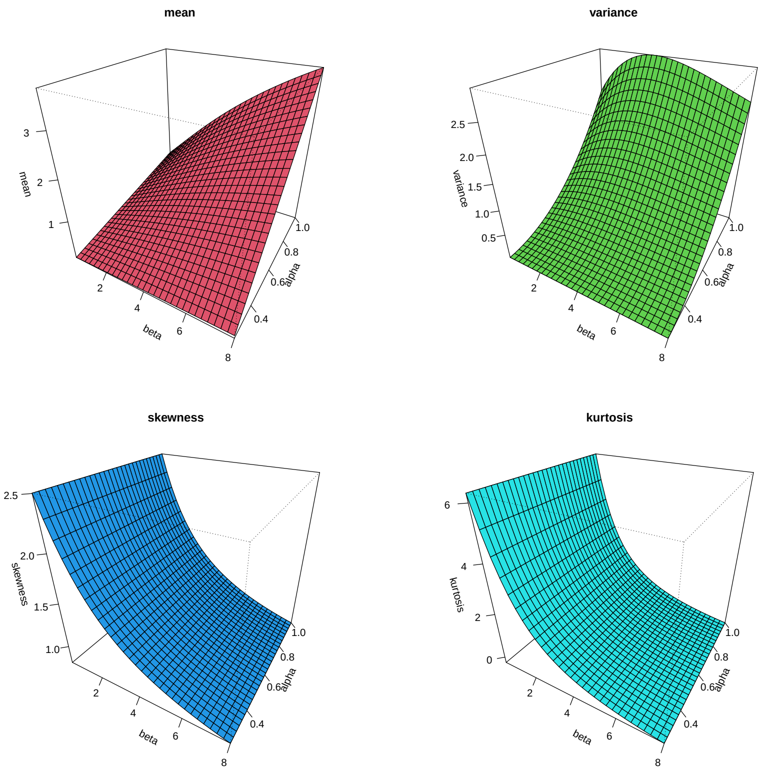

Figure 6. Mathematical properties plots of the EPD at $\theta = 2$.

3.3. Distribution of order statistics

Consider a random sample of size n $Z_1, Z_2, ..., Z_n$ is taken from the EPD with the PDF and CDF given as Eqs (2.2) and (2.1), respectively. The PDF of the r^{th}-order statistics can be obtained as

$$r_{(i:n)}(z) = \frac{n!}{(i-1)!(n-i)!}\,\phi(z;\alpha,\beta,\theta)\,[\Phi(z;\alpha,\beta,\theta)]^{i-1}\,[1-\Phi(z;\alpha,\beta,\theta)]^{n-i}$$

$$= \frac{n!\alpha z^{\alpha-1}}{(i-1)!(n-i)!\beta^{\alpha}}\left[1+\theta\left(\frac{z}{\beta}\right)^{\alpha}\right] e^{-\theta\left(\frac{z}{\beta}\right)^{\alpha}}\left[1-\left(1-\left(\frac{z}{\beta}\right)^{\alpha}\right) e^{-\theta\left(\frac{z}{\beta}\right)^{\alpha}}\right]^{i-1}$$

$$\times\left[\left(1-\left(\frac{z}{\beta}\right)^{\alpha}\right) e^{-\theta\left(\frac{z}{\beta}\right)^{\alpha}}\right]^{n-i}.$$

In particular, the minimum first-order and maximum n^{th}-order statistics, denoted by $Z_{(1:n)}$ and $Z_{(n:n)}$, play a vital role. Therefore, the density of $Z_{(1:n)}$ and $Z_{(n:n)}$ for the EPD are obtained as follows:

$$r_{(1:n)}(z) = \frac{n\alpha z^{\alpha-1}}{\beta^{\alpha}}\left[1+\theta\left(\frac{z}{\beta}\right)^{\alpha}\right] e^{-\theta\left(\frac{z}{\beta}\right)^{\alpha}}\left[\left(1-\left(\frac{z}{\beta}\right)^{\alpha}\right) e^{-\theta\left(\frac{z}{\beta}\right)^{\alpha}}\right]^{n-1},$$

and

$$r_{(n:n)}(z) = \frac{n\alpha z^{\alpha-1}}{\beta^{\alpha}}\left[1+\theta\left(\frac{z}{\beta}\right)^{\alpha}\right] e^{-\theta\left(\frac{z}{\beta}\right)^{\alpha}}\left[1-\left(1-\left(\frac{z}{\beta}\right)^{\alpha}\right) e^{-\theta\left(\frac{z}{\beta}\right)^{\alpha}}\right]^{n-1}.$$

Finally, the i^{th} CDF of Z is given below

$$\begin{aligned}R_{(i:n)}(z) &= \sum_{m=i}^{n} \Phi^{m}(z,\alpha,\beta,\theta)\,[1-\Phi(z;\alpha,\beta,\theta)]^{n-m}\\ &= \sum_{m=i}^{n}\left[1-\left(1-\left(\frac{z}{\beta}\right)^{\alpha}\right) e^{-\theta\left(\frac{z}{\beta}\right)^{\alpha}}\right]^{m}\left[\left(1-\left(\frac{z}{\beta}\right)^{\alpha}\right) e^{-\theta\left(\frac{z}{\beta}\right)^{\alpha}}\right]^{n-m}.\end{aligned}$$

4. Estimation methods

In this section, we estimate the models' parameters using two estimation techniques, namely maximum likelihood estimation and Bayesian methods.

4.1. Maximum likelihood estimation

Consider a random sample $(z_1, z_2, \ldots, z_n)$ taken from the EPD. The log-likelihood for the EPD, $\mathcal{LL}(z;\boldsymbol{\eta})$ with $\boldsymbol{\eta} = (\alpha,\beta,\theta)$, is given by

$$\mathcal{LL}(z;\boldsymbol{\eta}) = \sum_{i=1}^{n}\log\phi(z_i;\boldsymbol{\eta}) = n\log\alpha - n\alpha\log\beta + (\alpha-1)\sum_{i=1}^{n}\log(z_i) + \sum_{i=1}^{n}\log\left[1+\theta\left(\frac{z_i}{\beta}\right)^{\alpha}\right] - \theta\sum_{i=1}^{n}\left(\frac{z_i}{\beta}\right)^{\alpha}. \quad (4.1)$$

The components of the score vector,

$$U(\boldsymbol{\eta}) = \frac{\partial\mathcal{LL}(z;\boldsymbol{\eta})}{\partial\boldsymbol{\eta}} = \left(\frac{\partial\mathcal{LL}(z;\boldsymbol{\eta})}{\partial\alpha}, \frac{\partial\mathcal{LL}(z;\boldsymbol{\eta})}{\partial\beta}, \frac{\partial\mathcal{LL}(z;\boldsymbol{\eta})}{\partial\theta}\right)^{T},$$

are available if needed. Setting $U(\boldsymbol{\eta}) = 0$ and solving them simultaneously yields the MLEs of $\boldsymbol{\eta}$. The non-linear equations thus obtained are

$$\frac{\partial\mathcal{LL}(z;\boldsymbol{\eta})}{\partial\alpha} = \frac{n}{\alpha} - n\log\beta + \sum_{i=1}^{n}\log(z_i) + \theta\sum_{i=1}^{n}\frac{\left(\frac{z_i}{\beta}\right)^{\alpha}\log\left(\frac{z_i}{\beta}\right)}{1+\theta\left(\frac{z_i}{\beta}\right)^{\alpha}} - \theta\sum_{i=1}^{n}\left(\frac{z_i}{\beta}\right)^{\alpha}\log\left(\frac{z_i}{\beta}\right),$$

$$\frac{\partial\mathcal{LL}(z;\boldsymbol{\eta})}{\partial\beta} = -\frac{n\alpha}{\beta} - \alpha\theta\beta^{-1}\sum_{i=1}^{n}\frac{\left(\frac{z_i}{\beta}\right)^{\alpha}}{1+\theta\left(\frac{z_i}{\beta}\right)^{\alpha}} + \theta\alpha\beta^{-1}\sum_{i=1}^{n}\left(\frac{z_i}{\beta}\right)^{\alpha},$$

and

$$\frac{\partial\mathcal{LL}(z;\boldsymbol{\eta})}{\partial\theta} = \sum_{i=1}^{n}\frac{\left(\frac{z_i}{\beta}\right)^{\alpha}}{1+\theta\left(\frac{z_i}{\beta}\right)^{\alpha}} - \sum_{i=1}^{n}\left(\frac{z_i}{\beta}\right)^{\alpha}.$$

These equations cannot be solved analytically, and statistical software including R software's can be used to solve them numerically via iterative methods (Newton_Raphson or fixed_point techniques).

4.2. Bayesian technique

Let α, β, and θ be random variables following a gamma distribution with the parameters a_1, b_1, a_2, b_2, a_3, and b_3.

$$\pi_1(\alpha) = \frac{b_1^{a_1}}{\Gamma(a_1)}\, \alpha^{a_1-1}\, e^{-b_1\alpha}, \quad \alpha, a_1, b_1 > 0,$$

$$\pi_2(\beta) = \frac{b_2^{a_2}}{\Gamma(a_2)}\, \beta^{a_2-1}\, e^{-b_2\beta}, \quad \beta, a_2, b_2 > 0,$$

and

$$\pi_3(\theta) = \frac{b_3^{a_3}}{\Gamma(a_3)}\, \theta^{a_3-1}\, e^{-b_3\theta}, \quad \theta, a_3, b_3 > 0.$$

The joint density function will be

$$\pi(\boldsymbol{\eta}) = \frac{b_1^{a_1}}{\Gamma(a_1)}\, \frac{b_2^{a_2}}{\Gamma(a_2)}\, \frac{b_3^{a_3}}{\Gamma(a_3)}\, \alpha^{a_1-1}\, \beta^{a_2-1}\, \theta^{a_3-1}\, e^{-b_1\alpha-b_2\beta-b_3\theta}.$$

The joint prior density of $\boldsymbol{\eta}$ and the complete samples are given below:

$$\begin{aligned}\pi^*(\boldsymbol{\eta} \mid z) &= \mathcal{L}(\boldsymbol{\eta})\pi(\boldsymbol{\eta}) \\ &= \frac{b_1^{a_1}}{\Gamma(a_1)}\, \frac{b_2^{a_2}}{\Gamma(a_2)}\, \frac{b_3^{a_3}}{\Gamma(a_3)}\, \alpha^{n+a_1-1}\, \beta^{a_2-\alpha n-1}\, \theta^{a_3-1}\, e^{-b_1\alpha-b_2\beta-b_3\theta} \prod_{i=1}^{n} z_i^{\alpha-1} \left[1+\theta\left(\frac{z_i}{\beta}\right)^{\alpha}\right] e^{-\theta\left(\frac{z_i}{\beta}\right)^{\alpha}}.\end{aligned}$$

Consequently, the Bayes estimator-based square error (SE) loss function $R = (\eta-\hat{\eta})^2$ can be established as follows:

$$\hat{R}_{SE} = \int_{\eta} R\, \pi^*(\eta \mid z)\, d\eta. \tag{4.2}$$

It is difficult to obtain analytical expressions of Eq (4.2). To solve this issue, we have considered the Metropolis Hasting (MH) algorithm.

5. Simulation experiments

This section presents the findings of a detailed Monte Carlo simulation study to evaluate the performance of the derived estimation approaches.

Numerically and using the average estimates (AE), average biases (AB), and mean squared errors (MSE), we can perform simulation experiments to assess the finite sample behavior of the MLEs and Bayes techniques. The assessment was based on $N = 1000$ replications for all ($n = 25, 50, 75, 100$) and various parameter values (Set 1: (α,β,θ)=(1.2,0.2,1.1); Set 2: (α,β,θ)=(1.3,0.75,1.2); Set 3: (α,β,θ)=(1.5,1,1.3); Set 4: (α,β,θ)=(1.7,1.5,1)). The proposed criteria for the estimated parameters denoted as $\boldsymbol{\eta} = (\alpha,\beta,\theta)$ are detailed below:

$$\mathrm{AE} = \frac{1}{N}\sum_{i=1}^{N} \widehat{\boldsymbol{\eta}}, \qquad \mathrm{AB} = \frac{1}{N}\sum_{i=1}^{N} |\widehat{\boldsymbol{\eta}} - \boldsymbol{\eta}|, \qquad \mathrm{MSE} = \frac{1}{N}\sum_{i=1}^{N} (\widehat{\boldsymbol{\eta}} - \boldsymbol{\eta})^2.$$

To obtain a random sample from the EPD, the following algorithm is considered: (1) Generate p from $U \sim (0, 1)$; (2) Find z as follows:

$$z = \beta \left\{ 1 - \frac{1}{\theta} W \left[\theta \, e^{\theta} (1 - p) \right] \right\}^{\frac{1}{\alpha}}.$$

The consistency of the estimators obtained by MLE and Bayes methods are seen in Tables 3–7, where Figures 7–9 report the MSE plots for the unknown parameters of the proposed EPD using the the two suggested estimation techniques. The following are evident from Tables 3–7 and Figures 7–10:

(1) The average estimate values across the two estimation approaches converge to the initial value as n rises.
(2) The Bayesian estimation approach provides the closest estimates for all choices of α, β, and θ.
(3) The MLE method often shows a higher average bias and mean square error.
(4) The Bayesian technique tends to perform efficiently for estimating the unknown parameters of the EPD.
(5) For the time complexity, the Bayesian method is quicker than MLE for computing the final estimates of the model parameters.

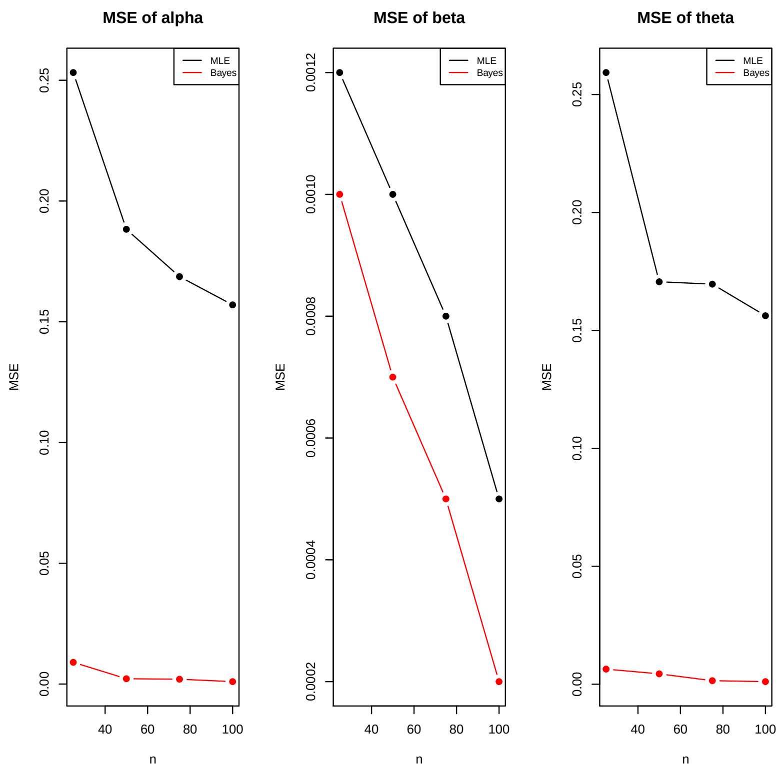

Figure 7. MSE plots of α, β, and θ under the two estimation techniques using Set 1.

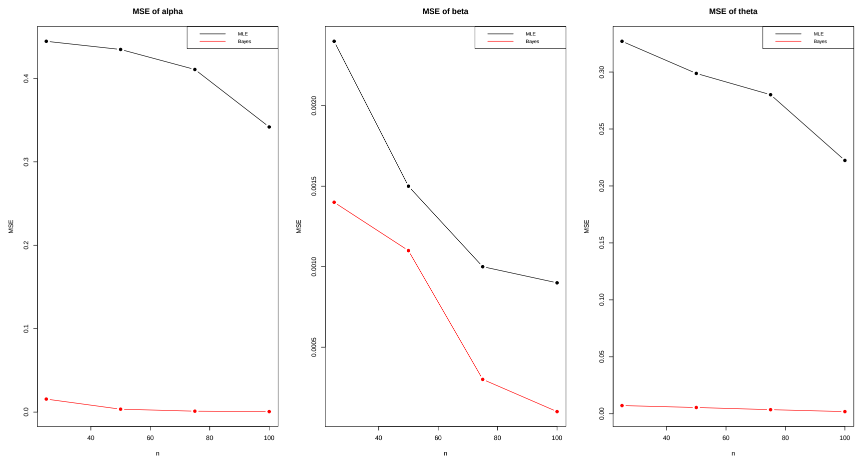

Figure 8. MSE plots of α, β, and θ under the two estimation techniques using Set 2.

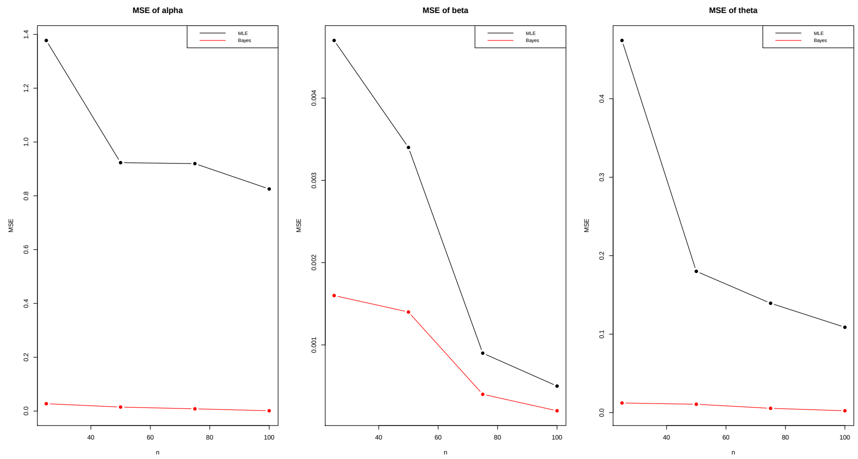

Figure 9. MSE plots of α, β, and θ under the two estimation techniques using Set 3.

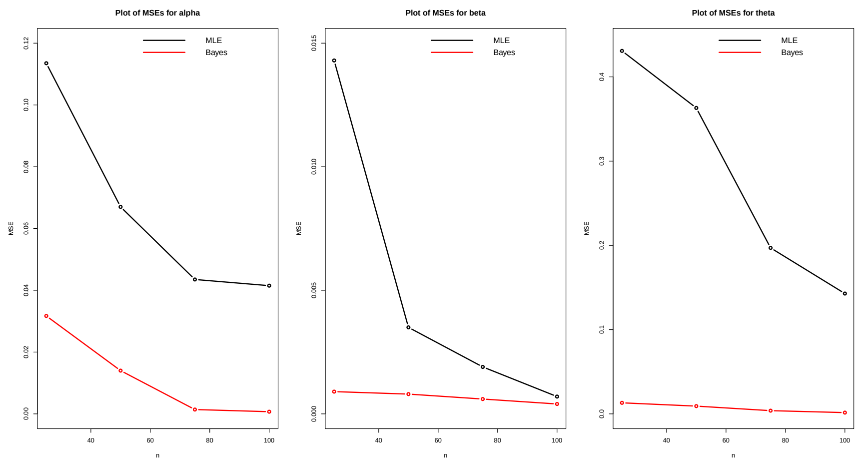

Figure 10. MSE plots of α, β, and θ under the two estimation techniques using Set 4.

Table 3. Estimates of the parameter based on the MLE and Bayes estimators using Set 1.

n		$\hat{\alpha}$			$\hat{\beta}$			$\hat{\theta}$		
		AE	AB	MSE	AE	AB	MSE	AE	AB	MSE
25	MLE	1.6534	0.4534	0.2532	0.1766	0.0234	0.0012	1.1389	0.0389	0.2593
	Bayes	1.1877	0.0123	0.0090	0.2537	0.0537	0.0010	1.1135	0.0135	0.0064
50	MLE	1.4356	0.2356	0.1883	0.1910	0.0090	0.0010	0.8641	0.2359	0.1706
	Bayes	1.1534	0.0466	0.0022	0.1930	0.0070	0.0007	1.0629	0.0371	0.0044
75	MLE	1.5883	0.3883	0.1687	0.1937	0.0063	0.0008	1.3416	0.2416	0.1696
	Bayes	1.2470	0.0470	0.0020	0.2046	0.0046	0.0005	1.1214	0.0214	0.0015
100	MLE	1.5872	0.3872	0.157	0.1967	0.0033	0.0005	1.2740	0.1740	0.1562
	Bayes	1.1683	0.0317	0.0010	0.1991	0.0009	0.0002	1.1061	0.0061	0.0011

Table 4. Estimates of the parameter based on the MLE and Bayes estimators using Set 2.

n		$\hat{\alpha}$			$\hat{\beta}$			$\hat{\theta}$		
		AE	AB	MSE	AE	AB	MSE	AE	AB	MSE
25	MLE	2.1133	0.8133	0.4445	0.7028	0.0472	0.0024	1.1878	0.0122	0.327
	Bayes	1.1767	0.1233	0.0156	0.7335	0.0165	0.0014	1.1687	0.0313	0.0072
50	MLE	1.9352	0.6352	0.4347	0.7281	0.0219	0.0015	1.6381	0.4381	0.2988
	Bayes	1.2407	0.0593	0.0035	0.6680	0.0820	0.0011	1.2381	0.0381	0.0055
75	MLE	1.8625	0.5625	0.4107	0.7291	0.0209	0.0010	1.4213	0.2213	0.2801
	Bayes	1.2672	0.0328	0.0011	0.7544	0.0044	0.0003	1.1735	0.0265	0.0036
100	MLE	1.7634	0.4634	0.3418	0.7313	0.0187	0.0009	1.5163	0.3163	0.2224
	Bayes	1.3077	0.0077	0.0006	0.7575	0.0075	0.0001	1.2001	0.0002	0.0019

Table 5. Estimates of the parameter based on the MLE and Bayes estimators using Set 3.

n		$\hat{\alpha}$			$\hat{\beta}$			$\hat{\theta}$		
		AE	AB	MSE	AE	AB	MSE	AE	AB	MSE
25	MLE	2.6283	1.1283	1.3774	0.9417	0.0583	0.0047	1.5247	0.2247	0.4743
	Bayes	1.4891	0.0109	0.0273	0.9599	0.0401	0.0016	1.2520	0.0480	0.0123
50	MLE	2.2228	0.7228	0.9232	0.9616	0.0384	0.0034	1.4823	0.1823	0.1801
	Bayes	1.4736	0.0264	0.0148	0.9630	0.0370	0.0014	1.2794	0.0206	0.0107
75	MLE	2.1394	0.6394	0.9196	0.9776	0.0224	0.0009	1.5006	0.2006	0.1394
	Bayes	1.5481	0.0481	0.0083	0.9385	0.0615	0.0004	1.2263	0.0737	0.0055
100	MLE	1.6931	0.1931	0.8254	0.9841	0.0159	0.0005	1.4740	0.1740	0.1088
	Bayes	1.5171	0.0171	0.0011	1.0189	0.0189	0.0002	1.2948	0.0052	0.0024

Table 6. Estimates of the parameter based on the MLE and Bayes estimators using Set 4.

n		$\hat{\alpha}$			$\hat{\beta}$			$\hat{\theta}$		
		AE	AB	MSE	AE	AB	MSE	AE	AB	MSE
25	MLE	1.7909	0.0909	0.1135	1.4219	0.0781	0.0143	0.7954	0.2046	0.4308
	Bayes	1.7169	0.0169	0.0317	1.5295	0.0295	0.0009	1.0676	0.0324	0.0131
50	MLE	1.7124	0.0124	0.0670	1.4653	0.0347	0.0035	0.8729	0.1271	0.3631
	Bayes	1.7374	0.0374	0.0140	1.5431	0.0431	0.0009	1.0227	0.0227	0.0092
75	MLE	1.7308	0.0308	0.0435	1.4642	0.0358	0.0019	0.8333	0.1667	0.1970
	Bayes	1.7370	0.0370	0.0014	1.5245	0.0245	0.0006	1.0106	0.0194	0.0038
100	MLE	1.6944	0.0056	0.0415	1.4783	0.0217	0.0007	0.9631	0.0369	0.1428
	Bayes	1.6801	0.0199	0.0007	1.5098	0.0098	0.0004	1.0111	0.0189	0.0015

Table 7. Summary of performance by the estimation method.

Estimator	Small *n* performance	Large *n* performance	Bias trend	MSE trend	Overall rank
Bayes	Excellent (lowest AB, MSE)	Excellent (best overall)	Low	Low	1^{st}
MLE	Moderate	Good	Moderate	Moderate	2^{nd}

6. Real data analysis

In this section, we illustrate the applicability, flexibility, and potentiality of the proposed EPD by analyzing four datasets from the medical science and insurance fields.

6.1. First dataset

The first dataset is about the mortality for COVID-19 in France from 1 January to 20 February 2021. The data originate from Almetwally [29]. The dataset is provided in Table 8.

Table 8. Values of COVID-19 in France.

0.0995	0.0525	0.0615	0.0455	0.1474	0.3373	0.1087	0.1055	0.2235	0.0633	0.0565	0.2577	0.1345
0.0843	0.1023	0.2296	0.0691	0.0505	0.1434	0.2326	0.1089	0.1206	0.2242	0.0786	0.0587	0.1516
0.2070	0.1170	0.1141	0.2705	0.0793	0.0635	0.1474	0.2345	0.1131	0.1129	0.2054	0.0600	0.0534
0.1422	0.2235	0.0908	0.1092	0.1958	0.0580	0.0502	0.1229	0.1738	0.0917	0.0787	0.1654	

6.2. Second dataset

Turning our attention to the second dataset, we delve into the mortality for COVID-19 in Canada. This data were sourced from the period 1 November to 26 December 2020, and it was studied by Nasiru et al. [30]. The data set is summarized in Table 9.

Table 9. Values of COVID-19 in Canada.

0.1622	0.1159	0.1897	0.1260	0.3025	0.2190	0.2075	0.2241	0.2163	0.1262	0.1627	0.2591	0.1989	0.3053	0.2170
0.2241	0.2174	0.2541	0.1997	0.3333	0.2594	0.2230	0.2290	0.1536	0.2024	0.2931	0.2739	0.2607	0.2736	0.2323
0.1563	0.2677	0.2181	0.3019	0.2136	0.2281	0.2346	0.1888	0.2729	0.2162	0.2746	0.2936	0.3259	0.2242	0.1810
0.2679	0.2296	0.2992	0.2464	0.2576	0.2338	0.1499	0.2075	0.1834	0.3347	0.2362				

6.3. Third dataset

The values of this data set were tokens from Saudi Arabia and represent current health expenditure in terms of economic growth rates. The proposed application was considered by Emam [31], and its records are reported in Table 10.

Table 10. The records of the third dataset.

42.1159410	44.6173573	42.4937630	39.7909737	35.8400607	34.1867280	36.1922503
35.6228733	29.7100425	42.9041958	36.4785600	37.1177721	40.1962376	44.6568298
52.2795486	59.9834490	58.3562946	62.6256323	57.4845695	56.8828773	

6.4. Fourth dataset

Here, the dataset was taken from a medical insurance group and represented one thousandth (1000^{th}) of the loss amount in euros (EUR) of all claims exceeding 25,000 USD in 1991. It is available at `http://www.soa.org` and also it is available in the *SOAGM* function () in the **CASdatasets** package [32] for R. For computational purposes, each observation of loss amount is divided by 1000, which is unlikely to affect the inference issues. In Figure 11, we have visualized all the proposed data set values as several non-parametric plots including time-sorted, box, and histogram plots. Further, to investigate potential outliers, we utilized kernel density, probability-probability (P-P) and quantile-quantile (Q-Q) plots for the four selected datasets, as depicted in Figure 12.

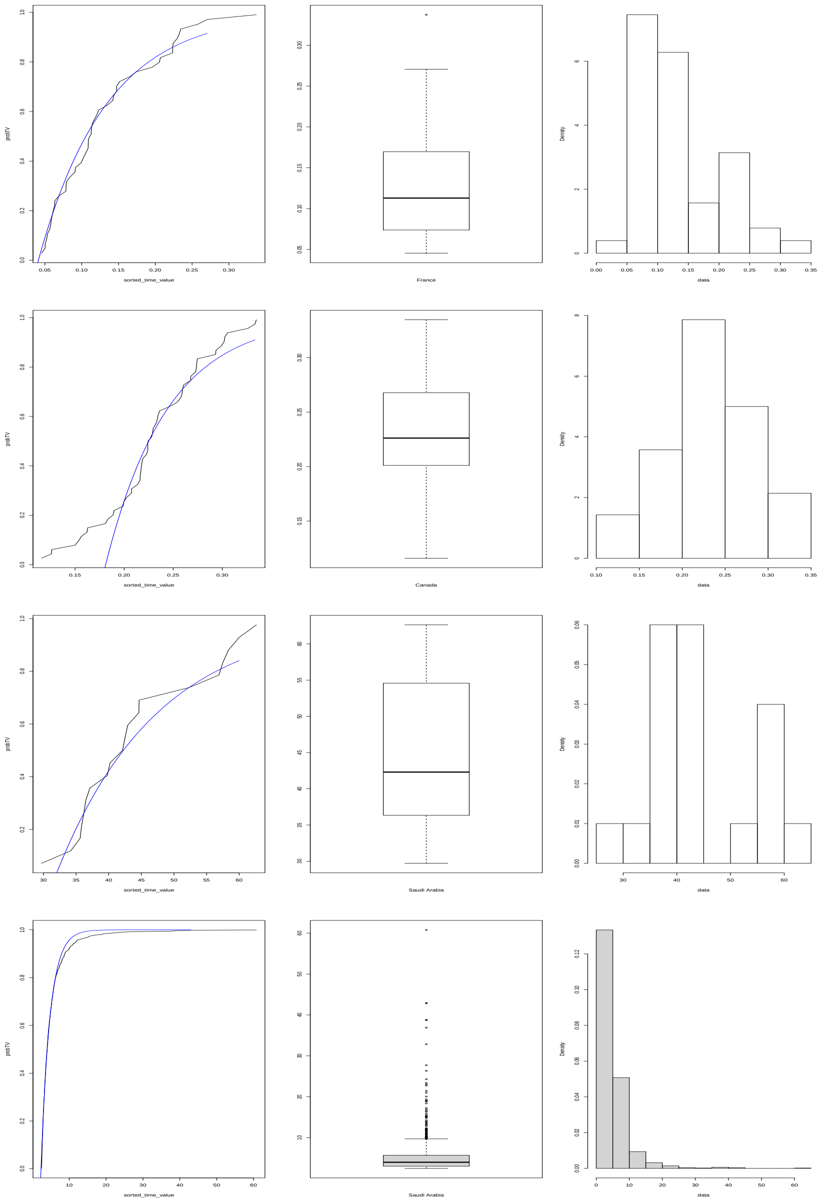

Figure 11. Time-sorted values, box, and histogram plots for the four datasets.

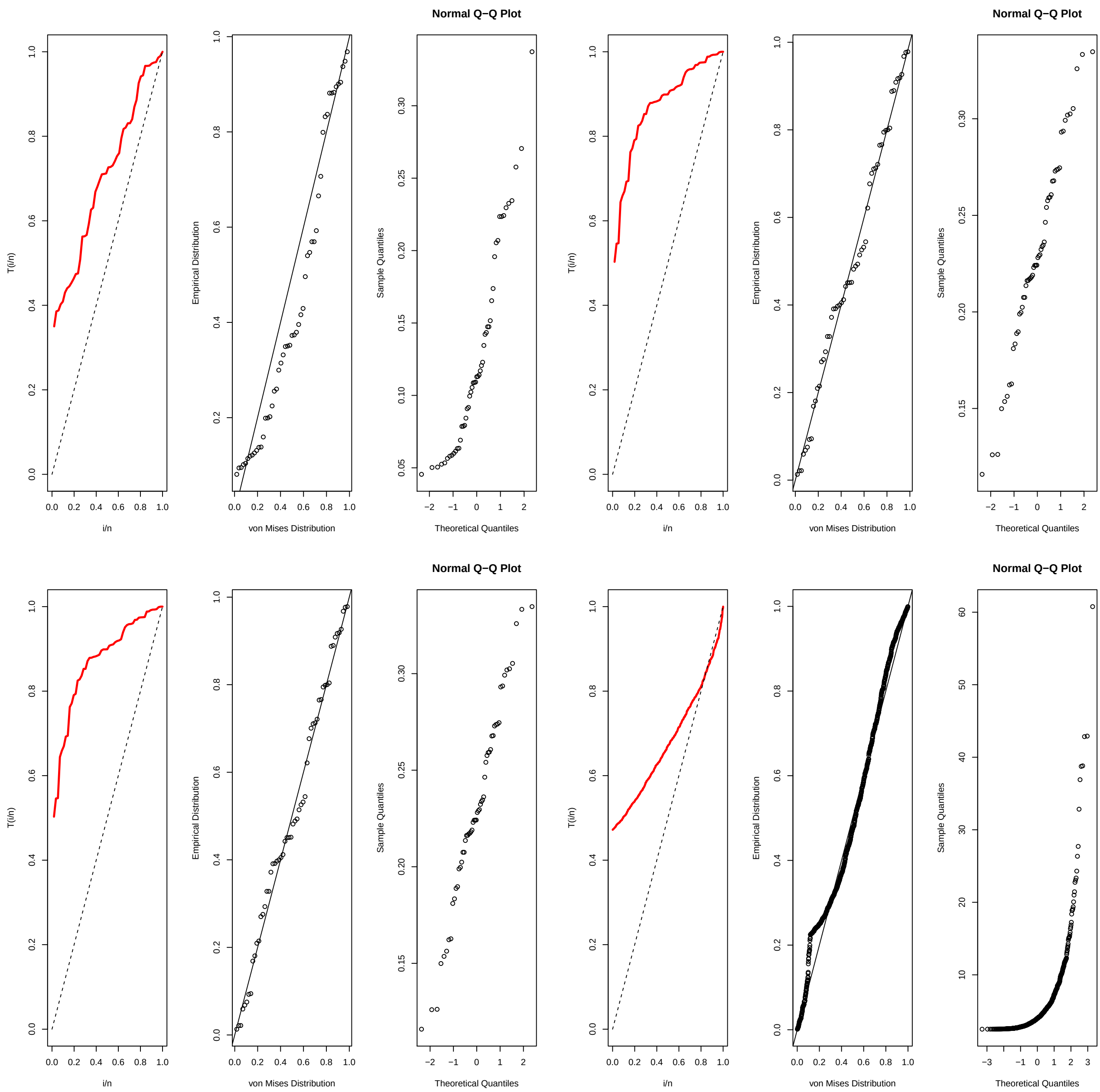

Figure 12. The total test time (TTT), PP, and Q-Q plots for the four datasets.

For a detailed comparison, we apply the EPD to the datasets along with several competitive distributions such as the exponential Weibull distribution (EWD), the modified Kies Gompertz (MKGO), the truncated Poisson power distribution (TPPD), the new exponential exponential distribution (NEED), the exponential TX Gompertz (EXTGO) distribution, the alpha power transformed exponential (APTE) distribution, the sine Nadaraja Haghighi (SNH) distribution, and the PD.

All these parameters are estimated using the MLE approach. We utilized the Akaike information criterion ($\mathcal{A}$), Bayesian information criterion ($\mathcal{B}$), and Kolmogorov_Smirnov goodness-of-fit metrics ($\mathcal{KS}$), and the associated $\mathcal{P}$-value to explore the fitting performance and selection of the best-fitting model. We present the analysis results in Table 11, which are illustrated in Tables 11 and 12. The numerical values of Tables 11 and 12 clearly lead to the inference that the EPD emerges as the preferred choice and could be deemed to be the best-fitting model for the four proposed data sets. Figures 13–17 show the empirical CDF, PDF, and survival plots for the four datasets. From these figures, we can observe that the EPD has the greatest degree of correspondence and representation with these data sets. Regarding the time complexity, the Bayesian method is quicker than MLE for computing the final estimates of the model parameters. Additionally, the empirical aggregate function, CDF, and SF functions for the new model and the comparison distributions demonstrate the superiority of the EPD over its counterparts.

Table 11. The parameter estimates and goodness-of-fit measures of all fitted distributions for the selected datasets.

Data	Distribution	$\hat{\alpha}$	$\hat{\beta}$	$\hat{\theta}$	$\mathcal{KS}$	$\mathcal{P}$-value	$\mathcal{A}$	$\mathcal{B}$
I	EPD	18.608	2.0158	164.55	0.1085	0.5846	103.62	109.42
	EWD	1.8170	28.955	231.13	0.1166	0.4915	104.57	110.36
	MKGO	1.4247	0.0182	24.094	0.1378	0.2873	108.03	113.83
	TPPD	41.107	1.5871	202.32	0.1500	0.2008	108.30	114.09
	NEED	0.0135	56.009		0.3013	0.0001	133.37	137.23
	PD	92.097	0.2188		0.5183	2.4×10^{-12}	269.79	273.65
	APTE	1.4846	30.433		0.1508	0.1962	106.271	110.135
	SNH	1.9417	0.2024		0.2696	0.0012	122.218	126.082
	ETXGO	1.1127	1.8821	0.0604	0.1229	0.4242	108.799	114.594
II	EPD	6.9723	5.0321	170.37	0.1028	0.5942	90.688	96.764
	EWD	4.2104	9.5876	293.60	0.1097	0.5096	93.501	99.577
	MKGO	3.2888	0.1013	2.3640	0.1232	0.3630	92.107	98.183
	TPPD	18.466	96.882	0.0049	0.5540	2.3×10^{-10}	292.56	298.63
	NEED	0.0762	4.6805		0.4085	1.5×10^{-08}	217.47	221.52
	PD	67.075	0.2702		0.5552	1.99×10^{-10}	343.84	347.89
	APTE	0.9478	136.173		0.266	0.0007	145.373	149.423
	SNH	1.6549	0.1430		0.4220	4.34×10^{-09}	193.738	197.789
	ETXGO	1.5810	0.0780	1.3629	0.1043	0.5746	269.79	104.536
III	EPD	4.9012	93.804	24.461	0.2115	0.2895	154.527	157.514
	EWD	225.431	3.2268	141.573	0.2266	0.2198	159.831	162.818
	MKGO	1.7720	3.1438	0.0957	0.3481	0.0113	170.017	173.005
	TPPD	62.695	0.0251	105.3479	0.2915	0.0532	156.838	159.825
	NEED	0.0045	4.0720		0.4747	0.0001	198.912	200.904
	PD	1.5650	83.168		0.3585	0.0082	177.577	179.569
	APTE	0.0461	62.134		0.3674	0.0062	174.971	176.963
	SNH	0.7170	0.0191		0.4778	0.0001	196.362	198.354
	ETXGO	7.0778	3.8051	0.0907	0.3304	0.0190	170.605	173.592

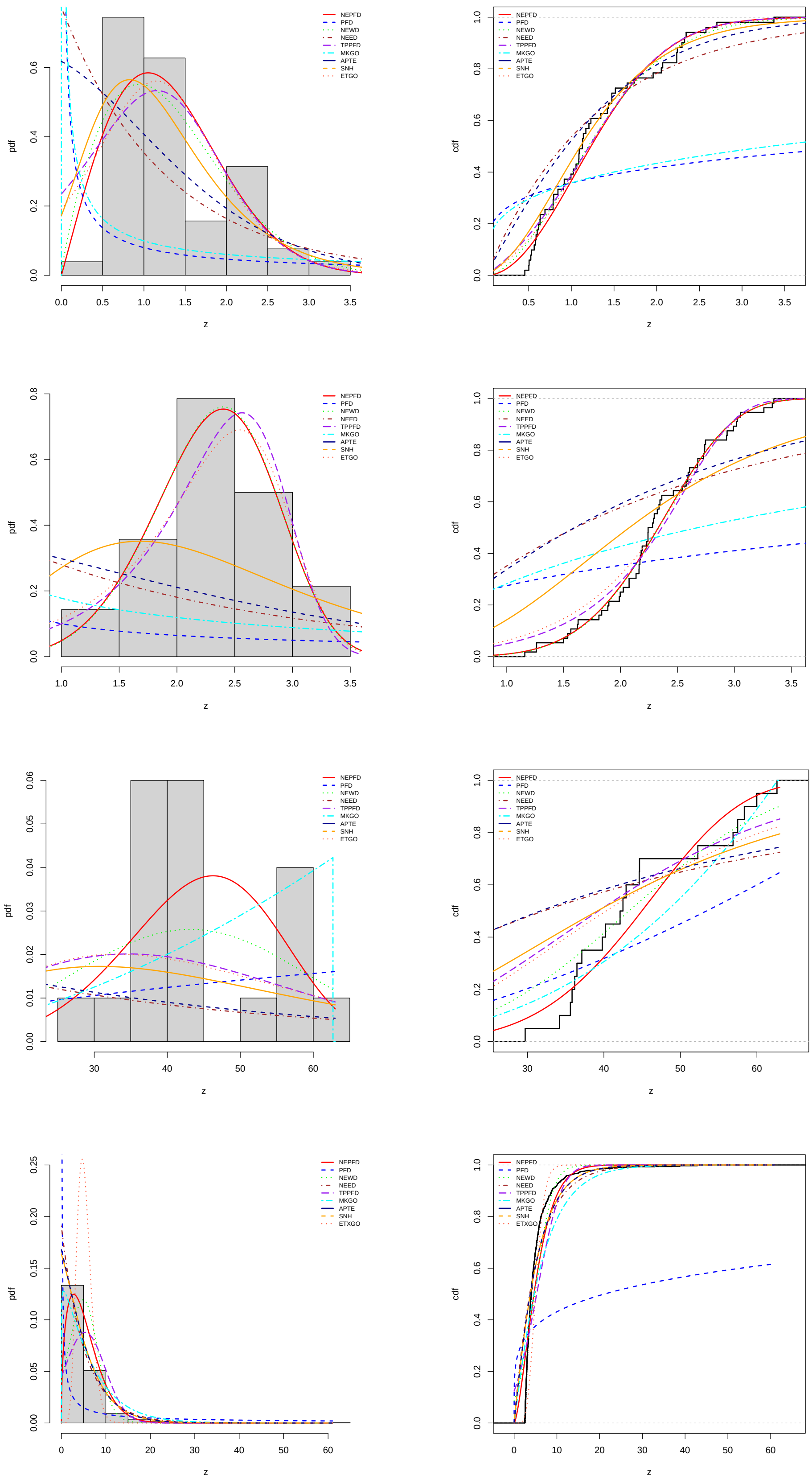

Figure 13. Fitted PDF and CDF for the compared models applying the selected datasets.

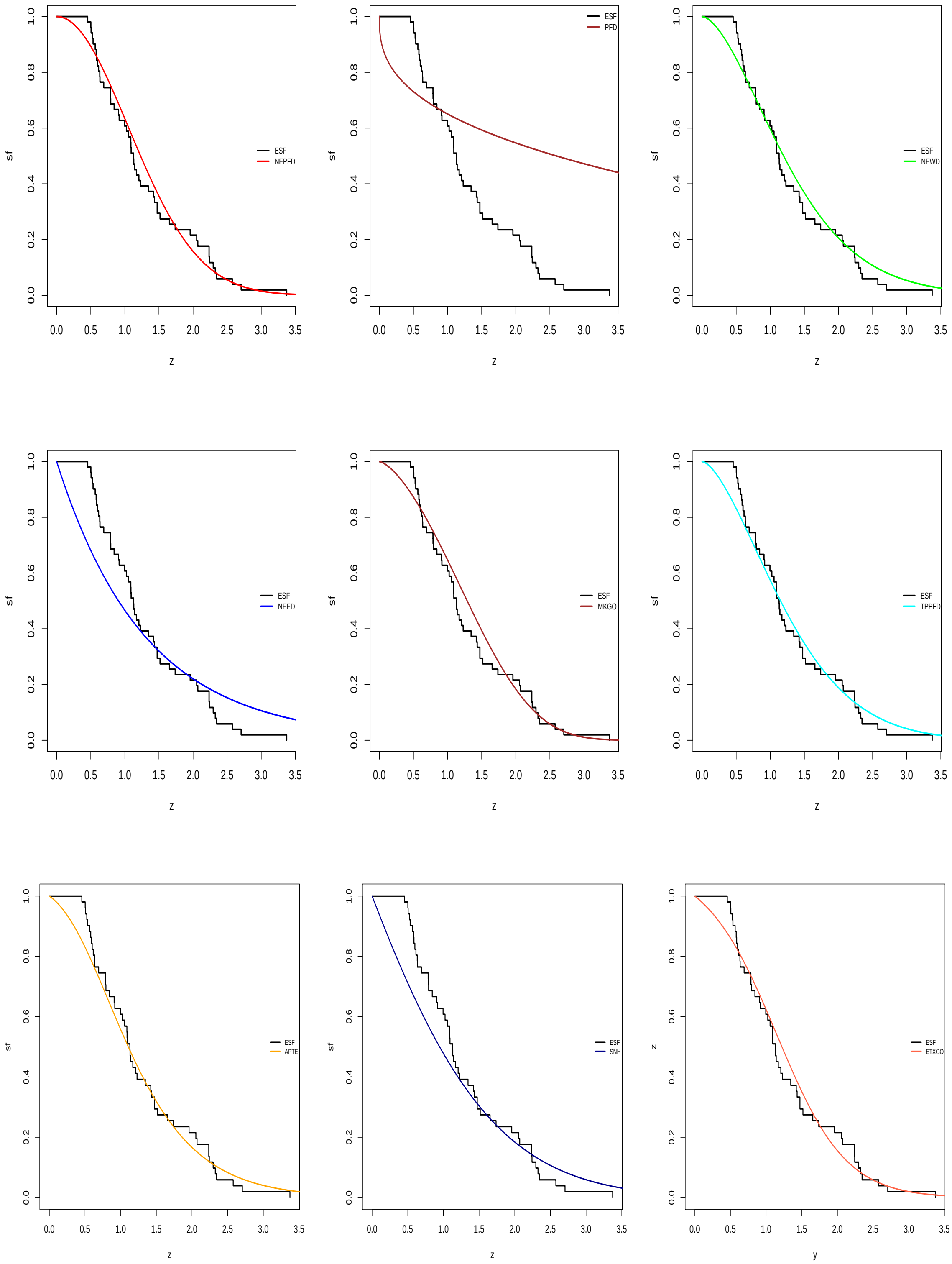

Figure 14. Fitted SFs for the compared models applied to the first dataset.

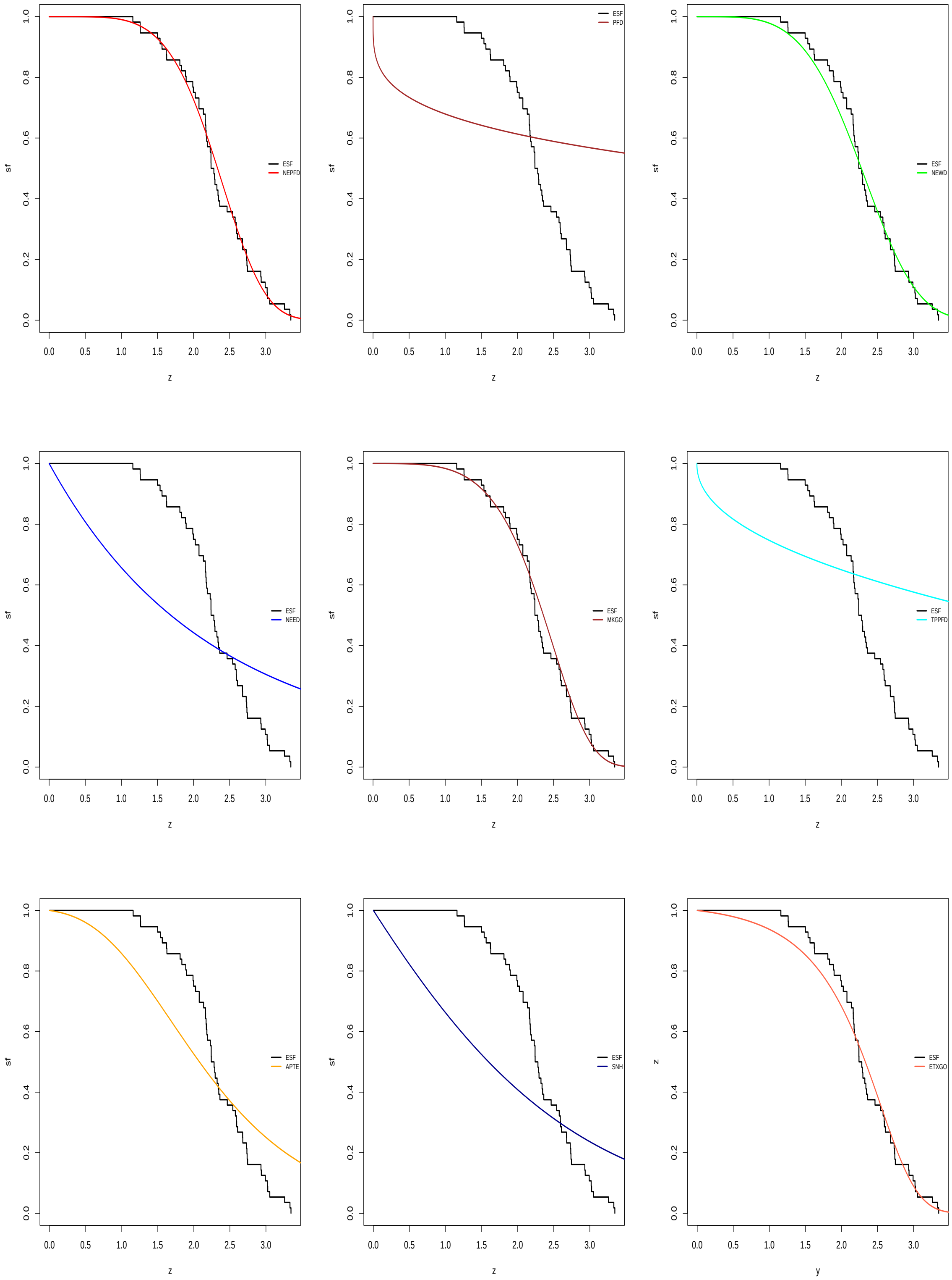

Figure 15. Fitted SFs for for the compared models applied to the second dataset.

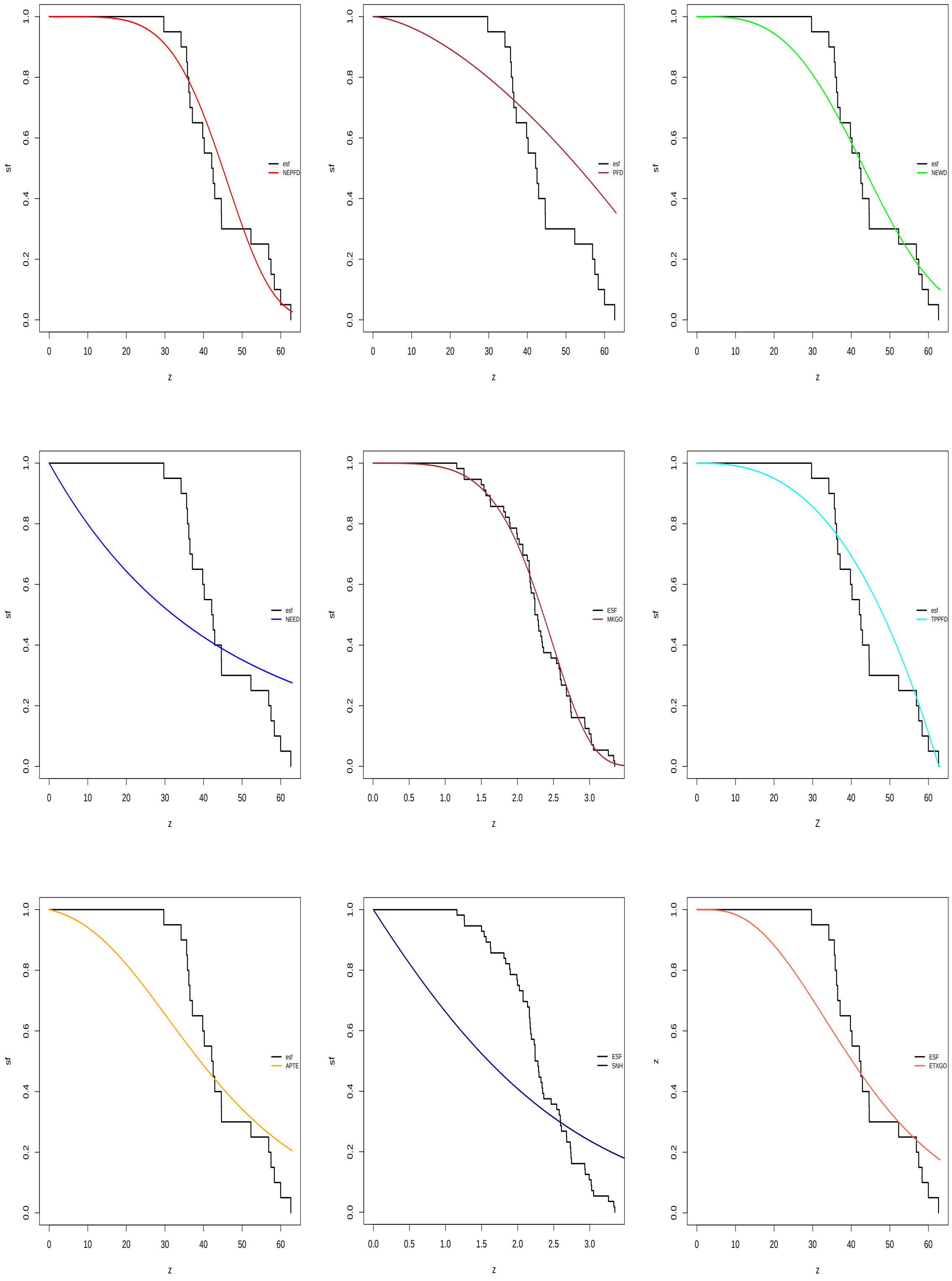

Figure 16. Fitted SFs for for the compared models applied to the third dataset.

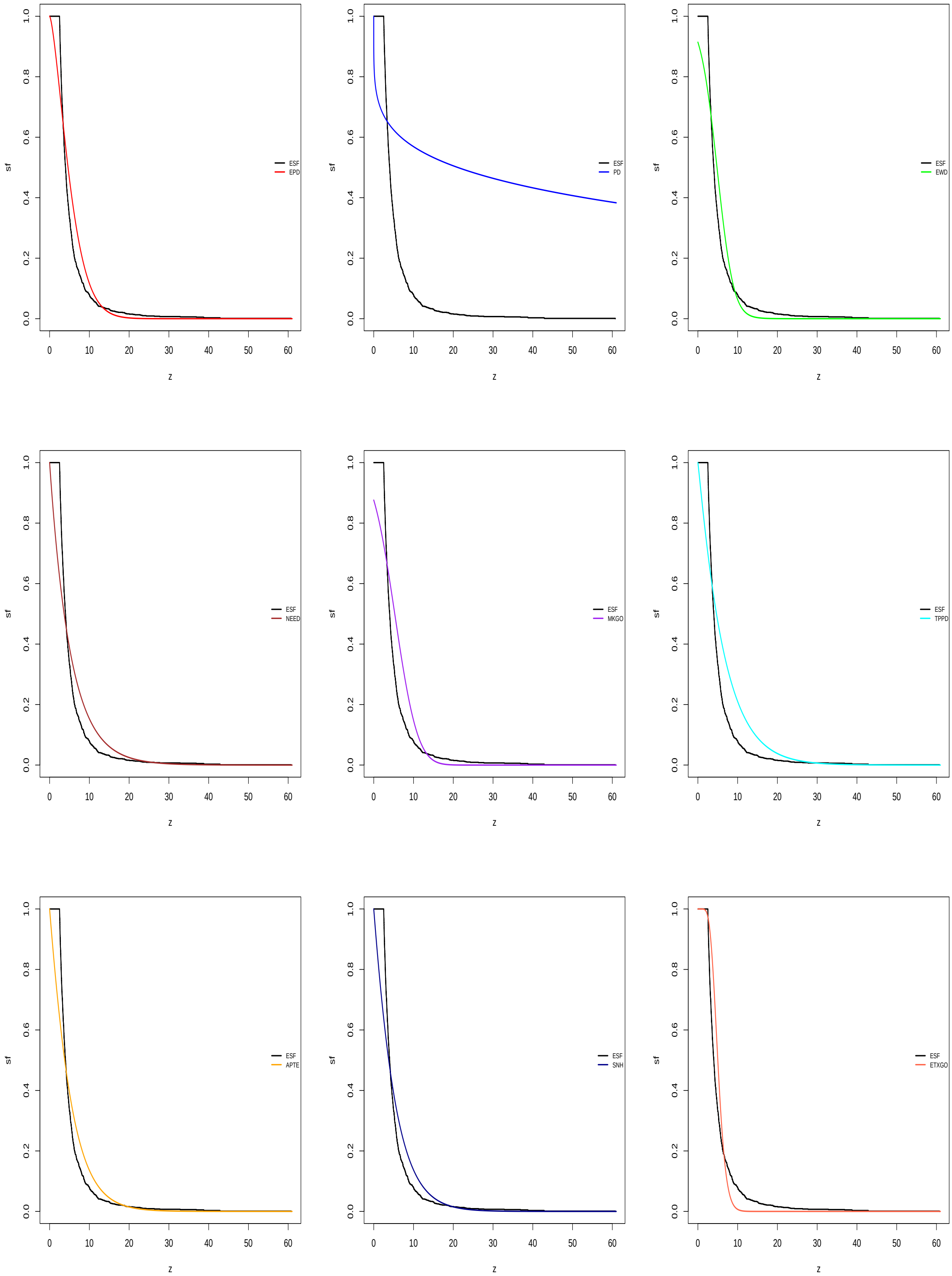

Figure 17. Fitted SFs for the compared models applied to the fourth dataset.

Table 12. The parameter estimates and goodness-of-fit measures of all fitted distributions for the fourth dataset.

Data	Distribution	$\hat{\alpha}$	$\hat{\beta}$	$\hat{\theta}$	$\mathcal{KS}$	$\mathcal{P}$-value	$\mathcal{A}$	$\mathcal{B}$
	EPD	1.4726	174.877	144.245	0.2439	0.1920	5063.91	5078.633
	EWD	4.9719	10.809	5.0314	0.2496	0.1846	5432.101	5446.824
	MKGO	14.446	5.0779	4.5444	0.2712	0.1320	5875.697	5890.420
IV	TPPD	74.552	1.0668	13.293	0.2995	0.1095	5311.853	5326.576
	NEED	0.0033	55.999		0.3786	0.00006	5347.796	5357.611
	PD	0.1982	698.248		0.5097	1.8×10^{-18}	8247.665	8257.481
	APTE	0.2251	1.8343		0.3582	0.0043	5253.753	5263.569
	SNH	1.0427	0.1024		0.3620	0.0008	5268.458	5278.274
	ETXGO	20.986	10.071	1.9626	0.1637	0.2588	5933.629	5948.352

7. Conclusions

We derived a novel three-parameter model known as the exponential power distribution (EPD) in this study, which is a new model using the NE method. We have developed numerous mathematical properties of the proposed model. Parameter estimation for the EPD is performed using maximum likelihood and Bayesian tools. We assessed the proposed estimators' finite sample behavior through simulation experiments using several statistical metrics. Our findings indicate that the Bayesian technique performs better than the MLE for estimating the unknown parameters. In the end, four applications were taken from the medical science and insurance fields to demonstrate the applicability of the proposed distribution, and it is shown that the EPD more efficiently analyzed both datasets. For future research, we can utilize this new model for other types of datasets, including skewed, bi-modal, and asymmetrical kinds, as well as applying it to discrete data and in reliability and environmental studies. We can also estimate the model parameters of the proposed EPD for the censoring type.

8. Limitations of the study

While our study demonstrates that the EPD is the best-fitting model, it is important to acknowledge that the EPD has certain disadvantages. For example, the EPD is used only for non discrete data. Moreover, its quantile function, moment, and associated measures have no closed form. As a result, we must use computer language to achieve random generation from the suggested distribution.

Author contributions

Muqrin did the writing and mathematics, and AbaOud did the revising, editing, and validating. All authors contributed equally to this paper. All authors have read and approved the final version of the manuscript for publication.

Use of Generative-AI tools declaration

The authors declare they have not used Artificial Intelligence (AI) tools in the creation of this article.

Acknowledgments

This work was supported and funded by the Deanship of Scientific Research at Imam Mohammad Ibn Saud Islamic University (IMSIU) (grant number IMSIU-DDRSP2501).

Funding

This work was supported and funded by the Deanship of Scientific Research at Imam Mohammad Ibn Saud Islamic University (IMSIU) (grant number IMSIU-DDRSP2501).

Conflict of interest

All authors declare no conflicts of interest in this paper.

References

1. H. Amal, G. N. Said, The inverse Weibull-G familiy, *J. Data Sci.*, 2018, 723–742.
2. M. A. Meraou, N. M. Al-Kandari, M. Z. Raqab, D. Kundu, Analysis of skewed data by using compound Poisson exponential distribution with applications to insurance claims, *J. Stat. Comput. Simul.*, **92** (2021), 928–956. https://doi.org/10.1080/00949655.2021.1981324
3. M. A. Meraou, N. M. Al-Kandari, M. Z. Raqab, Univariate and bivariate compound models based on random sum of variates with application to the insurance losses data, *J. Stat. Theory Pract.*, **16** (2022), 56. https://doi.org/10.1007/s42519-022-00282-8
4. A. Alzaatreh, C. Lee, F. Famoye, A new method for generating families of continuous distributions, *Metron*, **71** (2013), 63–79. https://doi.org/10.1007/s40300-013-0007-y
5. B. Thomas, V. M. Chacko, Power generalized DUS transformation in Weibull and Lomax distributions, *Reliab.: Theory Appl.*, **1** (2023), 368–384.
6. M. A. Meraou, M. Z. Raqab, D. Kundu, F. A. Alqallaf, Inference for compound truncated Poisson log-normal model with application to maximum precipitation data, *Commun. Stat. Simul. Comput.*, 2024, 1–22. https://doi.org/10.1080/03610918.2024.2328168
7. N. Eugene, C. Lee, F. Famoye, Beta-normal distribution and its applications, *Commun. Stat. Theory Methods*, **31** (2002), 497–512. https://doi.org/10.108/STA-120003130
8. G. M. Cordeiro, R. dos Santos Brito, The beta power distribution, *Braz. J. Probab. Stat.*, **26** (2012), 88–112. https://doi.org/10.1214/10-BJPS124
9. A. W. Marshall, I. Olkin, A new method for adding a parameter to a family of distributions with application to the exponential and Weibull families, *Biometrika*, **84** (1997), 641–652. https://doi.org/10.1093/biomet/84.3.641

10. E. M. Almetwally, M. A. Meraou, Application of environmental data with new extension of Nadarajah-Haghighi distribution, *Comput. J. Math. Stat. Sci.*, **1** (2022), 26–41. https://doi.org/10.21608/cjmss.2022.271186

11. Z. Ahmad, E. Mahmoudi, O. Kharazmi, On modeling the earthquake insurance data via a new member of the T-X family, *Comput. Intel. Neurosc.*, **2020** (2020), 7631495. https://doi.org/10.1155/2020/7631495

12. Z. Ahmad, E. Mahmoudi, S. Dey, S. K. Khosa, Modeling vehicle insurance loss data using a new member of T-X family of distributions, *J. Stat. Theory Appl.*, **19** (2020), 133–147. https://doi.org/10.2991/jsta.d.200421.001

13. W. He, Z. Ahmad, A. Z. Afify, H. Goual, The arcsine exponentiated-X family: validation and insurance application, *Complexity*, **2020** (2020), 8394815. https://doi.org/10.1155/2020/8394815

14. M. Meniconi, D. M. Barry, The power function distribution: a useful and simple distribution to assess electrical component reliability, *Microelectron. Reliab.*, **36** (1996), 1207–1212. https://doi.org/10.1016/0026-2714(95)00053-4

15. E. S. A. ElSherpieny, E. M. Almetwally, The exponentiated generalized alpha power family of distribution: properties and applications, *Pak. J. Stat. Oper. Res.*, **18** (2022), 349–367. https://doi.org/10.18187/pjsor.v18i2.3515

16. C. Wang, H. Zhu, Tests of fit for the power function lognormal distribution, *PLoS One*, **19** (2024), e0298309. https://doi.org/10.1371/journal.pone.0298309

17. H. M. Almongy, E. M. Almetwally, A. E. Mubarak, Marshall-Olkin alpha power Lomax distribution: estimation methods, applications on physics and economics, *Pak. J. Stat. Oper. Res.*, **17** (2021), 137–153. https://doi.org/10.18187/pjsor.v17i1.3402

18. E. Alshawarbeh, M. Z. Arshad, M. Z. Iqbal, M. Ghamkhar, A. Al Mutairi, M. A. Meraou, et al., Modeling medical and engineering data using a new power function distribution: theory and inference, *J. Radiat. Res. Appl. Sci.*, **17** (2024), 100787. https://doi.org/10.1016/j.jrras.2023.100787

19. E. A. Elsherpieny, A. Abdel-Hakim, Statistical analysis of Alpha-Power exponential distribution using unified Hybrid censored data and its applications, *Comput. J. Math. Stat. Sci.*, **4** (2025), 283–315.

20. E. F. Muhi, N. Oleiwi, N. Al-khairullah, A new family of power function-lindley distribution, *Adv. Nonlinear Var. Inequal.*, **27** (2024), 325–337.

21. M. Ahsan-ul-Haq, M. A. Aldahlan, J. Zafar, H. W. Gómez, A. Z. Afify, H. A. Mahra, A new cubic transmuted power-function distribution: properties, inference, and applications, *PLoS One*, **18** (2023), e0281419. https://doi.org/10.1371/journal.pone.0281419

22. M. H. Tahir, M. Alizadeh, M. Mansoor, G. M. Cordeiro, M. Zubair, The Weibull-power function distribution with applications, *Hacettepe J. Math. Stat.*, **45** (2016), 245–265.

23. E. M. Almetwally, Marshall Olkin alpha power extended Weibull distribution: different methods of estimation based on type I and type II censoring, *Gazi Univ. J. Sci.*, **35** (2022), 293–312. https://doi.org/10.35378/gujs.741755

24. E. Hussam, R. Alharbi, E. M. Almetwally, B. Alruwaili, A. M. Gemeay, F. H. Riad, Single and multiple ramp progressive stress with binomial removal: practical application for industry, *Math. Probl. Eng.*, **2022** (2022), 9558650. https://doi.org/10.1155/2022/9558650

25. D. Bolatova, S. Kadyrov, A. Kashkynbayev, Mathematical modeling of infectious diseases and the impact of vaccination strategies, *Math. Biosci. Eng.*, **21** (2024), 7103–7123. https://doi.org/10.3934/mbe.2024314

26. K. Velten, D. M. Schmidt, K. Kahlen, *Mathematical modeling and simulation: introduction for scientists and engineers*, John Wiley & Sons, 2024.

27. F. H. Riad, E. Hussam, A. M. Gemeay, R. A. Aldallal, A. Z. Afify, Classical and Bayesian inference of the weighted-exponential distribution with an application to insurance data, *Math. Biosci. Eng.*, **19** (2022), 6551–6581. https://doi.org/10.3934/mbe.2022309

28. S. Wang, W. Chen, M. Chen, Y. Zhou, Maximum likelihood estimation of the parameters of the inverse Gaussian distribution using maximum rank set sampling with unequal samples, *Math. Popul. Stud.*, **30** (2023), 1–21. https://doi.org/10.1080/08898480.2021.1996822

29. E. M. Almetwally, Application of COVID-19 pandemic by using odd lomax-G inverse Weibull distribution, *Math. Sci. Lett.*, **10** (2021), 47–57. https://doi.org/10.18576/msl/100203

30. S. Nasiru, A. G. Abubakari, C. Chesneau, New lifetime distribution for modeling data on the unit interval: properties, applications and quantile regression, *Math. Comput. Appl.*, **27** (2022), 105. https://doi.org/10.3390/mca27060105

31. W. Emam, Benefiting from statistical modeling in the analysis of current health expenditure to gross domestic product, *AIMS Math.*, **8** (2023), 12398–12421. https://doi.org/10.3934/math.2023623

32. C. Dutang, A. Charpentier, CASdatasets: insurance datasets, 2019. Available from: `https://dutangc.perso.math.cnrs.fr/RRepository/`.